Supplement of Atmos. Chem. Phys., 24, 9019–9030, 2024
https://doi.org/10.5194/acp-24-9019-2024-supplement

Atmospheric Chemistry and Physics
Open Access

Supplement of

Cooling radiative forcing effect enhancement of atmospheric amines and mineral particles caused by heterogeneous uptake and oxidation

Weina Zhang et al.

Correspondence to: Taicheng An (antc99@gdut.edu.cn)

S1：Free energy profile calculations

Free energy profile of each amine accumulated onto Kao surface is calculated with weighted histogram analysis method(Kumar et al., 1995) based on umbrella sampling from MD trajectory of each amine. Herein, Kao($Al_2Si_2O_5(OH)_4$) bulk is made up of an AlO_6 octahedral sheet and a SiO_4 tetrahedral sheet(Tenney and Cygan, 2014). (001) surface of Kao containing 1530 atoms is constructed in the box of 26.0×26.9×22.1 $Å^3$. A vacuum layer of 30 Å is added above equilibrated Kao surface along the Z-direction to avoid the interferences from circumambient mirror images. Single amine molecule is placed above 20 Å from the mass center of Kao. Configurations of amine-Kao are further equilibrated in *NVT*-MD for 500 ps. To investigate heterogeneous uptake process form air onto Kao surface, each amine molecule is moved by a step of 1.0 Å. At the updated position of amine molecule in each window, amine-Kao system is re-equilibrated within 250 ps and subsequently sampled within another 250 ps in *NVT* ensemble at 1 fs timestep. 21 windows are set to describe transport path of amine molecule from air to the mass center of Kao surface. Based on the MD results of each window, free energy profile of amine-Kao molecule is calculated by the umbrella sampling(Torrie and Valleau, 1997) and weighted with the histogram analysis method.(Roux, 1995; Kumar et al., 1995) The bias potential force constant is equal to 10 $kcal \cdot mol^{-1}$.(Martins-Costa et al., 2015; Martins-Costa et al., 2012) The final free energy profile is shown in Fig. S1A. The structure of amine-Kao with the lowest free energy indicates the adsorption site of amines on Kao surface.

S2： Simple forcing efficiency

Simple forcing efficiency (SFE) proposed by Bond and Bergstrom(Bond and Bergstrom, 2007) is calculated to quantify the influence of heterogeneous oxidation mechanisms on RFE of amine-Kao mixed particle. SFE is obtained from formula (1):

$$SFE=\frac{S_0}{4}\tau_{atm}^2(1-F_c)[2(1-a_s)^2\beta\cdot MSC-4a_s\cdot MAC] \quad (S1)$$

where S_0 is solar irradiance, τ_{atm} is atmospheric transmittance, F_c is cloud fraction, a_s is surface albedo, β is backscattering coefficient. Under the same atmospheric conditions, S_0, τ_{atm}, F_c, a_s and β keep constant. MSC and MAC are scattering and absorption cross section area per unit mass of mixed particles, respectively. Thereinto, the relationship between p and MAC is described as(Yang et al., 2022):

$$p=\frac{\rho\lambda MAC(\lambda)}{4\pi} \quad (S2)$$

where ρ and λ is the particle density and the wavelength of light, respectively. Herein, all the values of p for initial and oxidized amine-Kao particles are smaller than 0.002, which can be ignored. MAC is thus estimated to be zero. Therefore, light adsorption of amine-Kao mixed particle is not considered in evaluating RFE.

The relationship between n and MSC is determined by formula (S3)(Bond and Bergstrom, 2007):

$$MSC=\frac{4\pi^4 d^3 V}{M\lambda}\left(\frac{n^2-1}{n^2+2}\right)^2 \quad (S3)$$

where d, V, and M is the diameter, volume and M of amine-Kao particle, and λ is the wavelength of light.

To roughly estimate changes in SFE resulted from increased n, ΔSFE is defined as the ratio of SFE of amine-Kao particle to that of Kao. Note the changes in mass, volume

and diameter changes of particles during oxidation process are not considered.

45 Therefore, which is described as follows:

$$\Delta SFE=\frac{SFE_{amine\text{-}Kao}-SFE_{Kao}}{SFE_{Kao}}=\frac{MSC_{amine\text{-}Kao}}{MSC_{Kao}}-1=\frac{\left(\frac{n^2_{amine\text{-}Kao}-1}{n^2_{amine\text{-}Kao}+2}\right)^2}{\left(\frac{n^2_{Kao}-1}{n^2_{Kao}+2}\right)^2}-1 \qquad (S4)$$

S3：Figures and table of SI.

Table. S1. Summarized $\Delta E^{\neq}$, ΔE_r and k values for each reaction step of amine at 298 K. For energy barrier reaction, *ki* is calculated based on $\Delta E^{\neq}$, and for energy barrierless reactions, *ki* is calculated based on ΔE_r.

No.	Reaction	*T(K)*	$\triangle E^{\neq}$ *(kcal/mol)*	$\triangle E_r$ *(kcal/mol)*	*ki*	*Unit of k*
R1	MA+·OH→MA-·Rc+H_2O	298	-15.09	-22.50	1.27×10^{5}	s^{-1} $molec^{-1}$ cm^3
R2	DMA+·OH→DMA-·Rc+H_2O	298	-9.42	-23.33	9.22	s^{-1} $molec^{-1}$ cm^3
R3	TMA+·OH→TMA-·Rc+H_2O	298	2.75	-19.16	1.65×10^{-8}	s^{-1} $molec^{-1}$ cm^3
R4	MA+·OH→MA-·R_N+H_2O	298	-6.96	-13.42	1.24×10^{-1}	s^{-1} $molec^{-1}$ cm^3
R5	DMA+·OH→DMA-·R_N+H_2O	298	-6.26	-15.60	1.54×10^{-2}	s^{-1} $molec^{-1}$ cm^3
R6	MA-Rc+O_2→MA-RO_2·	298	/	-15.71	8.24×10^{4}	s^{-1} $molec^{-1}$ cm^3
R7	DMA-Rc+O_2→DMA-RO_2·	298	/	-17.90	3.32×10^{6}	s^{-1} $molec^{-1}$ cm^3
R8	TMA-Rc+O_2→TMA-RO_2·	298	/	-15.47	5.51×10^{4}	s^{-1} $molec^{-1}$ cm^3
R9	MA-RO_2·+NO→MA-RO·+NO_2	298	/	-4.70	7.08×10^{-4}	s^{-1} $molec^{-1}$ cm^3
R10	DMA-RO_2·+NO→DMA-RO·+NO_2	298	/	-33.91	1.79×10^{18}	s^{-1} $molec^{-1}$ cm^3
R11	TMA-RO_2·+NO→TMA-RO·+NO_2	298	/	-26.51	6.75×10^{12}	s^{-1} $molec^{-1}$ cm^3
R12	MA-RO·+O_2→NH_2CHO+HO_2	298	3.17	-58.74	4.30×10^{-9}	s^{-1} $molec^{-1}$ cm^3
R13	DMA-RO·+O_2→CH_3NHNHO+HO_2	298	4.91	-55.58	3.28×10^{-10}	s^{-1} $molec^{-1}$ cm^3

R14	TMA-RO·+O_2→$(CH_3)_2NCHO+HO_2$	298	3.22	-60.39	3.32×10^{-9}	s^{-1} $molec^{-1}$ cm^3
R15	MA-RO_2·→HN=CH2+HO_2	298	27.38	16.08	3.33×10^{-7}	s^{-1}
R16	DMA-RO_2·→$CH_3N=CH_2+HO_2$	298	21.16	7.54	4.98×10^{-3}	s^{-1}
R17	MA-RO_2·→·$NHCH_2OOH$ **(IM17)**	298	27.38	16.08	1.34×10^{-7}	s^{-1}
R18	DMA-RO_2·→·CH_2NHCH_2OOH**(IM18)**	298	19.61	13.66	1.85×10^{-1}	s^{-1}
R19	TMA-RO_2·→·$CH_2N(CH_3)CH_2OOH$**(IM19)**	298	14.15	9.47	2.23×10^{3}	s^{-1}
R20	·$NHCH_2OOH+O_2$**(RC20)**→$NH=CHOOH+HO_2$**(Pro20)**	298	5.79	-47.65	8.42×10^{-11}	s^{-1} $molec^{-1}$ cm^3
R21	·$CH_2NHCH_2OOH+O_2$**(RC21)**→·$OOCH_2NHCH_2OOH$**(IM21)**	298	/	-31.73	4.51×10^{16}	s^{-1} $molec^{-1}$ cm^3
R22	·$CH_2N(CH_3)CH_2OOH+O_2$**(RC22)**→·$OOCH_2N(CH_3)CH_2OOH$**(IM22)**	298	/	-14.49	1.05×10^{4}	s^{-1} $molec^{-1}$ cm^3
R23	·$OOCH_2NHCH_2OOH$**(IM21)**→$HOOCH_2NHCHO$+·OH	298	33.50	-41.69	1.00×10^{-11}	s^{-1}
R24	·$OOCH_2N(CH_3)CH_2OOH$**(IM22)**→$HOOCH_2N(CH_2·)CH_2OOH$**(IM24)**	298	12.93	7.71	1.72×10^{4}	s^{-1}
R25	$HOOCH_2N(CH_2·)CH_2OOH+O_2$**(RC25)**→$HOOCH_2N(CH_2OO·)CH_2OOH$**(IM25)**	298	/	-22.15	4.32×10^{9}	s^{-1} $molec^{-1}$ cm^3
R26	$HOOCH_2N(CH_2OO·)CH_2OOH$**(IM25)**→$(HOOCH_2)_2NCHO$+·OH	298	9.38	-52.18	4.20×10^{6}	s^{-1}
R27	MA-RO_2·+·OH→NH_2CH_2OOOH	298	/	-27.16	2.06×10^{13}	s^{-1} $molec^{-1}$ cm^3
R28	·$OOCH_2NHCH_2OOH$**(IM21)** +·OH→$HOOOCH_2NHCH_2OOH$	298	/	-32.06	8.06×10^{16}	s^{-1} $molec^{-1}$ cm^3

The rate constant for the reaction step with $\triangle E^{\neq} = 20$ kcal/mol is 1.38×10^{-2} s^{-1} (the first order reaction) and 5.68×10^{-22} s^{-1} $molec^{-1}$ cm^3 (the second order reaction).

Table. S2. Comparisons of $\triangle E^{\neq}$ and *k*i between homogeneous and heterogeneous oxidation reactions of MA, DMA and TMA.

Amine	No.	Heterogeneous oxidation (this work)		Homogeneous oxidation		Reference
		$\triangle E^{\neq}$ (kcal/mol)	*ki*	$\triangle E^{\neq}$ (kcal/mol)	*ki*	
MA	R1	-15.09	1.27×10^{5} s^{-1} $molec^{-1}$ cm^{3}	6.16(C-H)	1.88×10^{-11} s^{-1} $molec^{-1}$ cm^{3}	(Onel et al., 2013)
	R12	3.17	4.30×10^{-9} s^{-1} $molec^{-1}$ cm^{3}	/	/	
DMA	R2	-9.42	9.22 s^{-1} $molec^{-1}$ cm^{3}	8.46	6.39×10^{-11} s^{-1} $molec^{-1}$ cm^{3}	(Onel et al., 2013)
	R13	4.91	3.28×10^{-10} s^{-1} $molec^{-1}$ cm^{3}	/	/	
TMA	R3	2.75	1.65×10^{-8} s^{-1} $molec^{-1}$ cm^{3}	8.23	5.73×10^{-11} s^{-1} $molec^{-1}$ cm^{3}	(Onel et al., 2013)
	R14	3.22	3.32×10^{-9} s^{-1} $molec^{-1}$ cm^{3}	/	/	
	R19	14.15	2.23×10^{3} s^{-1}	17.8/16	2.9 s^{-1}	(Ma et al., 2021; Moller et al., 2020)
	R24	12.93	1.72×10^{4} s^{-1}	18.2/18.4	0.52 s^{-1}	(Ma et al., 2021; Moller et al., 2020)
	R26	9.38	4.20×10^{6} s^{-1}	20.1/18.1	5.1×10^{-2} s^{-1}	(Ma et al., 2021; Moller et al., 2020)

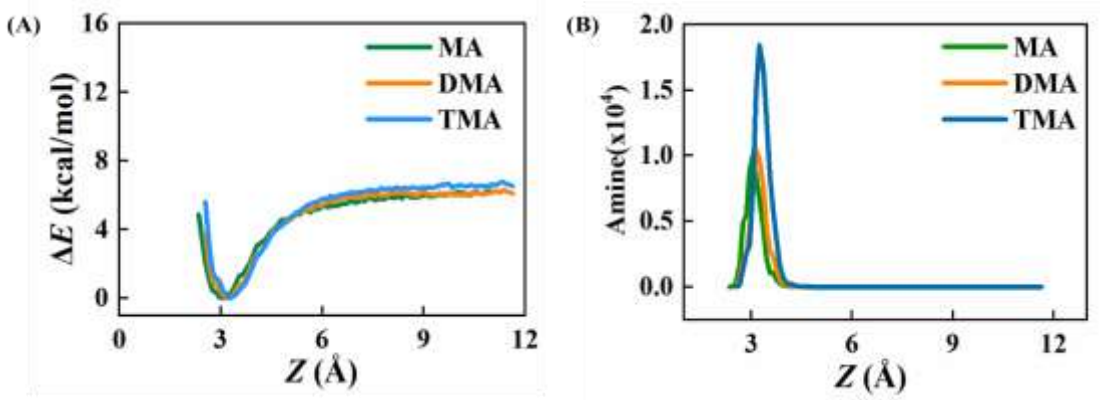

Fig. S1. Amine uptake by Kao particle simulated by classic MD simulation. (A) Free-energy profiles and (B) relative concentration changes of three amines accumulated on Kao surface.

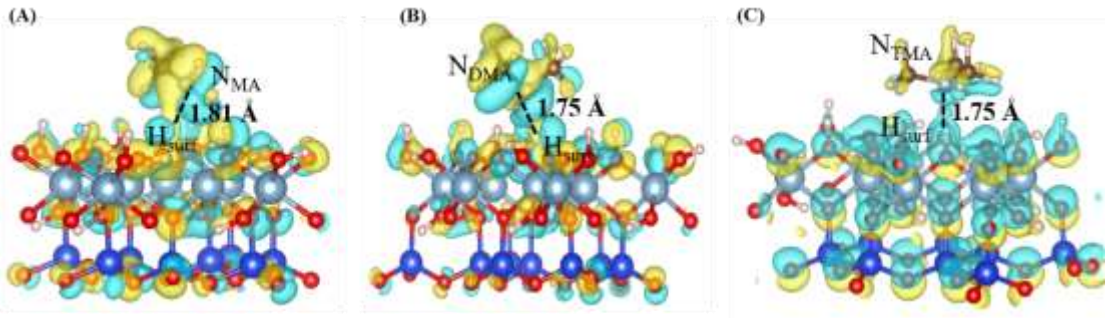

Fig. S2. Charge density differences and desorption energies of (A) MA-Kao, (B) DMA-Kao and (C) TMA-Kao mixed particles, respectively. Yellow and bule regions mean the regions where electron density increases and decreases, respectively.

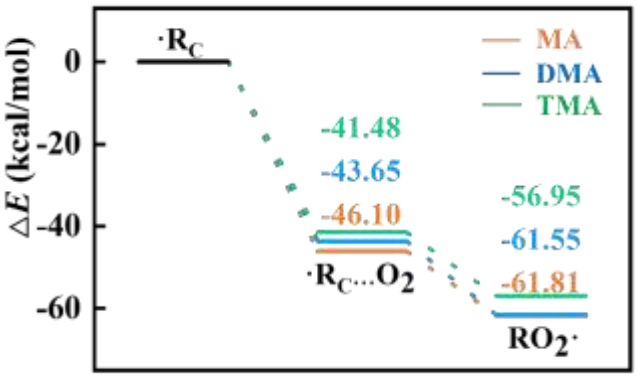

Fig. S3. PES of $R_C\cdot$ conversion into $RO_2\cdot$ on Kao surface.

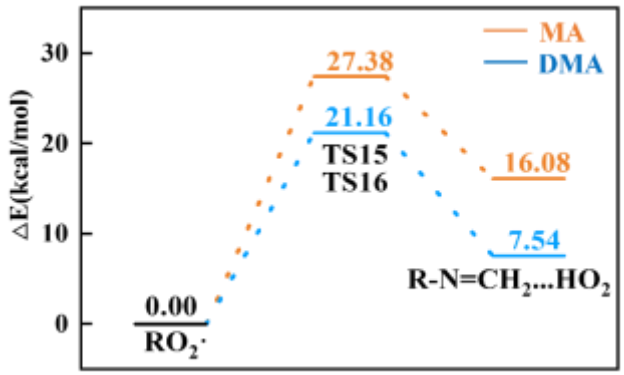

Fig. S4. PES of the H-abstraction reactions of MA's and DMA's $RO_2\cdot$ under clean condition.

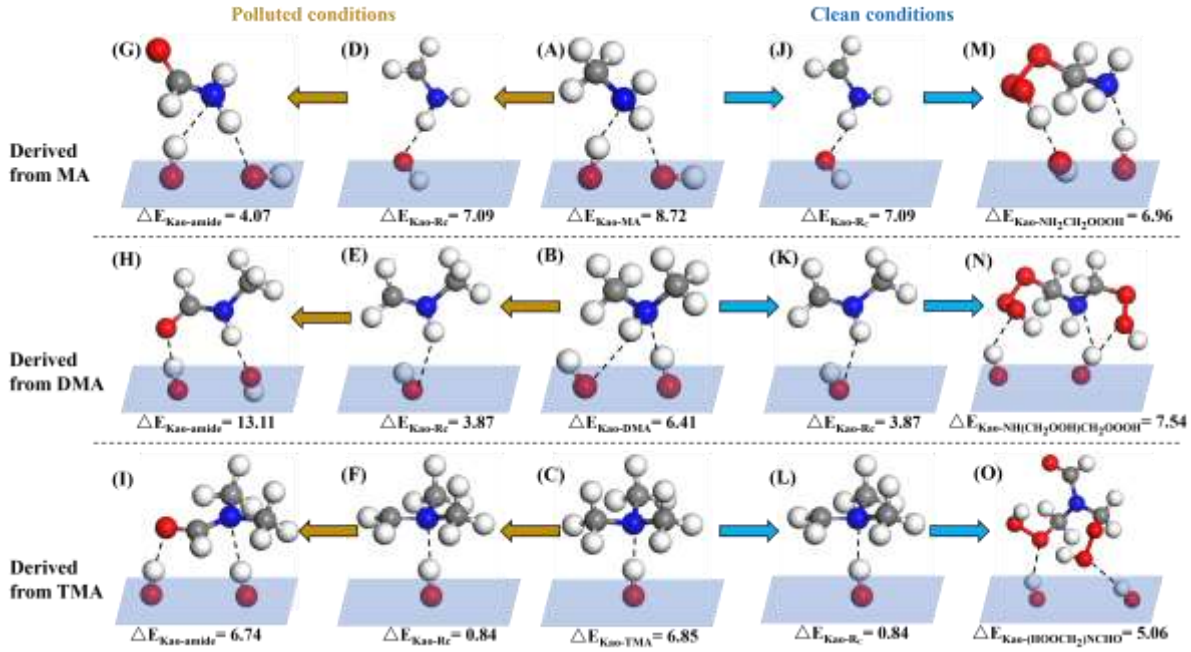

Fig. S5. All configurations and corresponding desorption energies of different amines and their oxidant products under polluted (brown arrows) and clean (blue arrows) conditions. (unit: kcal/mol)

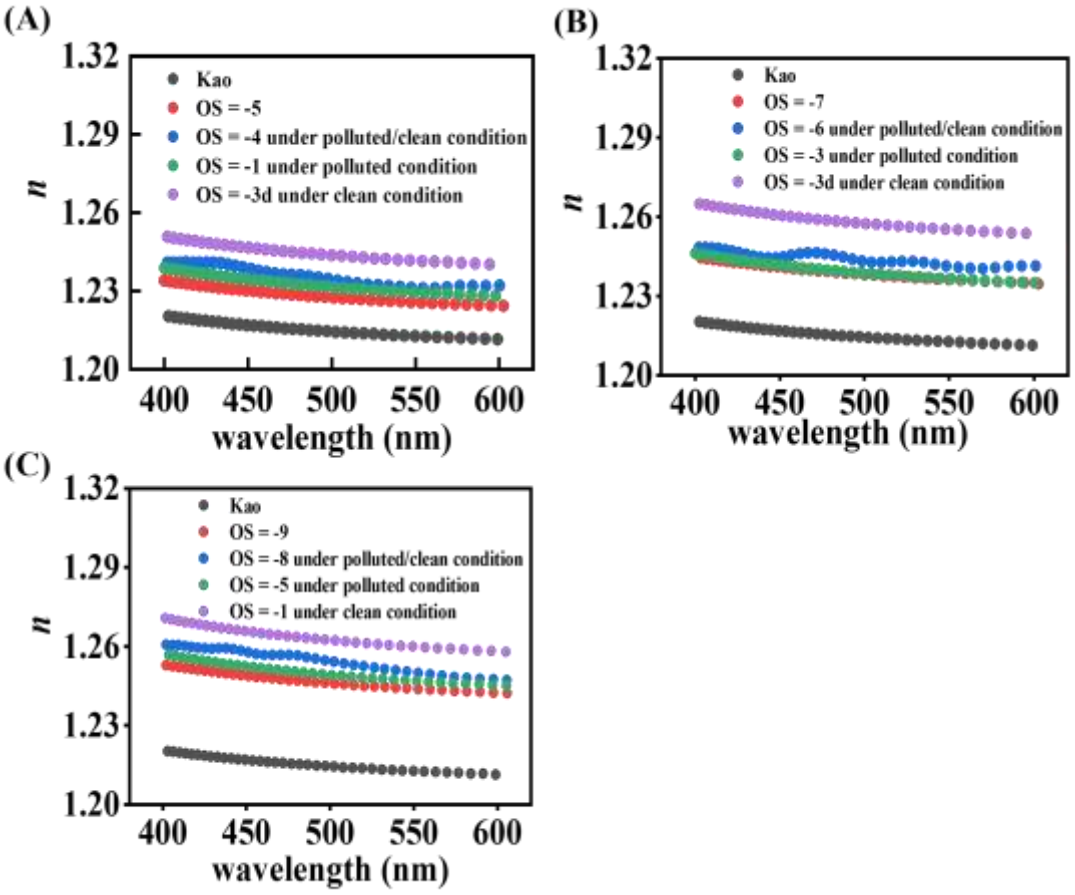

Fig. S6. *n* changes of each amine-Kao particle with increased wavelength (400 – 600 nm) under polluted and clean conditions. Results for (A) MA-Kao, (B) DMA-Kao or (C) TMA-Kao particles, respectively.

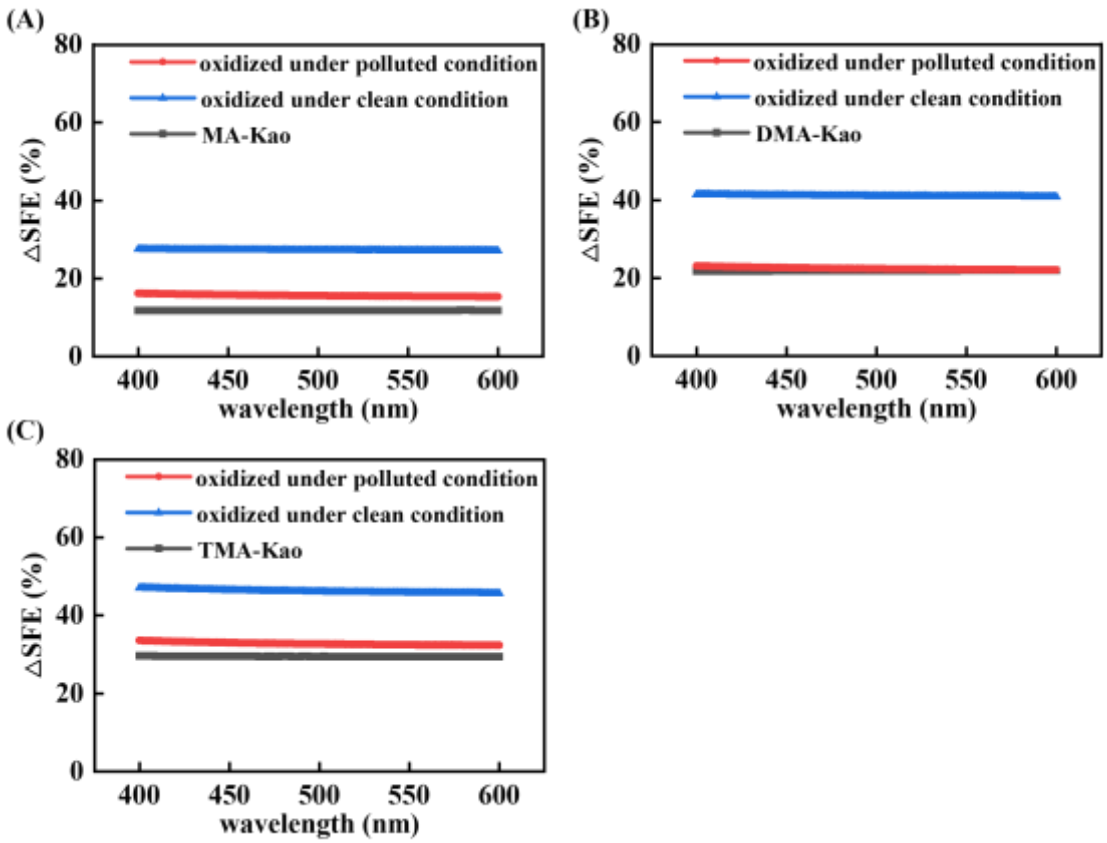

Fig. S7. ΔSFE profile of initial and oxidized (A) MA-Kao, (B) DMA-Kao and (C) TMA-Kao particles with increased wavelengths.

References in SI

Bond, T. C. and Bergstrom, R. W.: Light Absorption by Carbonaceous Particles: An Investigative Review, Aerosol Science and Technology, 40, 27-67, 10.1080/02786820500421521, 2007.

Kumar, S., Rosenberg, J. M., Bouzida, D., Swendsen, R. H., and Kollman, P.: Multidimensional free-energy calculations using the weighted histogram analysis method, J. Comput. Chem, 16, 1339-1350, 1995.

Ma, F., Xie, H. B., Li, M., Wang, S., Zhang, R., and Chen, J.: Autoxidation mechanism for atmospheric oxidation of tertiary amines: Implications for secondary organic aerosol formation, Chemosphere, 273, 129207, 10.1016/j.chemosphere.2020.129207, 2021.

Martins-Costa, M. T. C., García-Prietoa, F. F., and Ruiz-López, M. F.: Reactivity of aldehydes at the air–water interface. Insights from molecular dynamics simulations and ab initio calculations, Org. Biomol. Chem., 13, 1673, 2015.

Martins-Costa, M. T. C., Anglada, J. M., Francisco, J. S., and Ruiz-Lopez, M. F.: Reactivity of Volatile Organic Compounds at the Surface of a Water Droplet, J. Am. Chem. Soc., 134, 11821-11827, 10.1021/ja304971e, 2012.

Moller, K. H., Berndt, T., and Kjaergaard, H. G.: Atmospheric Autoxidation of Amines, Environ Sci Technol, 54, 11087-11099, 10.1021/acs.est.0c03937, 2020.

Onel, L., Thonger, L., Blitz, M. A., Seakins, P. W., Bunkan, A. J., Solimannejad, M., and Nielsen, C. J.: Gas-phase reactions of OH with methyl amines in the presence or absence of

molecular oxygen. An experimental and theoretical study, J Phys Chem A, 117, 10736-10745, 10.1021/jp406522z, 2013.
Roux, B.: The calculation of the potential of mean force using computer simulations, Comput. Phys. Comm., 91, 275-282, 1995.
Tenney, C. M. and Cygan, R. T.: Molecular Simulation of Carbon Dioxide, Brine, and Clay Mineral Interactions and Determination of Contact Angles, Environmental Science & Technology, 48, 2035-2042, 10.1021/es404075k, 2014.
Torrie, G. M. and Valleau, J. P.: Nonphysical sampling distributions in Monte Carlo free-energy estimation: Umbrella sampling, J. Comput. Phys., 23, 187, 1997.
Yang, Z., Tsona, N. T., George, C., and Du, L.: Nitrogen-Containing Compounds Enhance Light Absorption of Aromatic-Derived Brown Carbon, Environ Sci Technol, 56, 4005-4016, 10.1021/acs.est.1c08794, 2022.